2002

Development of a Novel CO Tolerant Proton Exchange Membrane Fuel Cell Anode

Andrew T. Haug
University of South Carolina - Columbia

Ralph E. White
University of South Carolina - Columbia, white@cec.sc.edu

John W. Weidner
University of South Carolina - Columbia, weidner@engr.sc.edu

Wayne Huang

Publication Info

Journal of the Electrochemical Society, 2002, pages A862-A867.

Publisher's link: http://dx.doi.org/10.1149/1.1479726
DOI: 10.1149/1.1479726

Journal of The Electrochemical Society, **149** (7) A862-A867 (2002)
0013-4651/2002/149(7)/A862/6/$7.00 © The Electrochemical Society, Inc.

Development of a Novel CO Tolerant Proton Exchange Membrane Fuel Cell Anode

Andrew T. Haug,[a,*] Ralph E. White,[a,] John W. Weidner,[a,***,z] and Wayne Huang[b]**

[a]*Center for Electrochemical Engineering, Department of Chemical Engineering, University of South Carolina, Columbia, South Carolina 29208, USA*
[b]*Plug Power, Incorporated, Latham, New York 12110, USA*
[c]*Energy and Environment Applications Center, Institute for Materials, School of Nanosciences and Engineering, State University of New York at Albany, Albany, New York 12203, USA*

Typically Pt is alloyed with metals such as Ru, Sn, or Mo to provide a more CO-tolerant, high-performance proton exchange membrane fuel cell (PEMFC) anode. In this work, a layer of carbon-supported Ru is placed between the Pt catalyst and the anode flow field to form a filter. When oxygen is added to the fuel stream, it was predicted that the slow H_2 kinetics of Ru in this filter would become an advantage compared to Pt and Pt:Ru alloy anodes, allowing a greater percentage of O_2 to oxidize adsorbed CO to CO_2. With an anode feed of H_2, 2% O_2, and up to 100 ppm CO, the Pt + Ru filter anode performed better at 70°C than the Pt:Ru alloy. The oxygen in the anode feed stream was found to form a hydroxyl species within the filter. The reaction of these hydroxyl groups with adsorbed CO was the primary means of CO oxidation within the filter. Because of the resulting proton formation, the Ru filter must be placed in front of and adjacent to the Pt anode and must contain Nafion in order to provide the ionic pathways for proton conduction, and hence achieve the maximum benefit of the filter.
 [DOI: 10.1149/1.1479726]

Manuscript submitted July 11, 2001; revised manuscript received January 11, 2002. Available electronically May 15, 2002.

Proton exchange membrane fuel cells (PEMFCs) are gaining popularity due to their benefits such as environmental friendliness and increased fuel efficiency. Because of the difficulties inherent to storing hydrogen, liquid fuels such as propane, natural gas, and gasoline are used to produce reformate gas. Dry reformate is typically composed of 35-45% hydrogen, 15-25% carbon dioxide, 50-10,000 ppm carbon monoxide, and a balance of nitrogen. It has been shown extensively that CO poisons the platinum catalyst used in PEMFC systems.[1-3] Carbon monoxide chemically adsorbs onto available Pt catalyst sites as shown in Eq. 1

$$CO + Pt \rightarrow CO_{ads} \quad [1]$$

At concentrations as low as 10 ppm, CO lowers power output of the PEMFC-containing Pt electrodes by 50%.[4,5] The addition of a preferential oxidation (PROX) unit to the fuel processing system can reduce CO concentrations in the reformate gas stream to approximately 50 ppm. Attempts to find catalysts both tolerant to CO and equivalent in performance to Pt have led to the alloying of Pt with Ru, Mo, W, Co, Ir, Ni, and Sn.[5-10] Used by themselves as anode catalysts, these metals do not provide the high rate of hydrogen oxidation necessary to achieve the current densities that make PEMFCs competitive in the marketplace.[7,11,12] The most commonly used alloy is Pt:Ru. The Pt:Ru alloys combine the high catalyst activity of Pt with the increased CO tolerance of Ru.[11-13]

The oxidation of CO_{ads} from the platinum catalyst surface in the anode shown in Eq. 2 has been found to follow Langmuir-Hinshelwood kinetics[11,12]

$$CO_{ads} + OH_{ads} \rightarrow CO_2 + H^+ + 2M + e^- \quad [2]$$

where M represents Pt or Ru. The reactions by which OH_{ads} is formed on Pt and Ru are shown in Eq. 3[14,15]

$$M + H_2O \rightarrow OH_{ads} + H^+ + e^- \quad [3]$$

The formation of OH_{ads}, shown in Eq. 3, is the rate-determining step of this reaction and occurs on platinum at potentials of 0.7 V/RHE and above.[12,14,15] Ruthenium has the ability to form OH_{ads} from water at significantly lower potentials than Pt, 0.35 V for 50 atom % Ru, and 0.2 V for 90 atom % Ru.[11,12,15] This allows the catalytic desorption of CO as CO_2 to commence at lower potentials. There is a linear relationship between the onset of CO oxidation and Ru composition (*i.e.*, the shift in potential is linear with respect to atomic fraction of Ru in the alloy). However, the benefit of alloying Pt with Ru has only been shown to provide near equivalent performance to pure H_2 on Pt for CO concentrations up to 100 ppm in the feed stream for low-temperature fuel cell PEMFC operation.[2,6]

The injection of oxygen into the fuel stream has also been shown to increase catalyst tolerance to CO.[13,16] This ''air bleeding'' provides a greater concentration of active oxygen on the catalyst that will then react with CO to form CO_2. The following reactions are assumed to occur at the Pt catalyst surface (in addition to Eq. 1)

$$O_2 + 2Pt \rightarrow 2O_{ads} \quad [4]$$

$$CO_{ads} + O_{ads} \rightarrow CO_2 + 2Pt \quad [5]$$

$$2H_{ads} + O_{ads} \rightarrow H_2O + 3Pt \quad [6]$$

The goal of the addition of an air bleed to the anode feed is to promote the reaction shown in Eq. 5, the oxidation of CO_{ads}, to CO_2. Note the difference between Eq. 2 and 5. The reaction of CO_{ads} with OH_{ads} on Pt requires an overpotential, and hence ionic contact to the cathode region (in the form of the Nafion electrolyte), whereas the reaction shown in Eq. 5 does not. One of the problems of adding O_2 to the gas inlet stream is that the reaction shown in Eq. 6 occurs at a much higher rate than the reaction shown in Eq. 5. Only about one of 400 O_2 molecules oxidizes CO_{ads} to CO_2.[13] This, and the fact that the mixture becomes combustible for concentrations of oxygen in hydrogen above 4 vol %, limits the amount of oxygen in the feed stream and limits the effectiveness of the air bleeding technique.

The first objective of this study was to determine if depositing a layer of carbon-supported Ru on top of a typical carbon-supported Pt anode (see Fig. 1) increases the effectiveness of the air-bleeding technique in preventing CO poisoning. By first coming in contact with Ru instead of Pt, it was speculated that a larger percentage of the O_2 in the $H_2/CO/O_2$ feed will react with CO_{ads} than in either a Pt or a Pt:Ru alloy electrode. The selectivity of Eq. 5 and 6 would then shift toward the oxidation of CO_{ads}. Studies have shown that the rate of hydrogen oxidation on pure Ru at 62°C (roughly the operating temperature used in this experiment) was two orders of magnitude lower than that of Pt measured under similar

* Electrochemical Society Student Member.
** Electrochemical Society Fellow.
*** Electrochemical Society Active Member.
z E-mail: weidner@engr.sc.edu

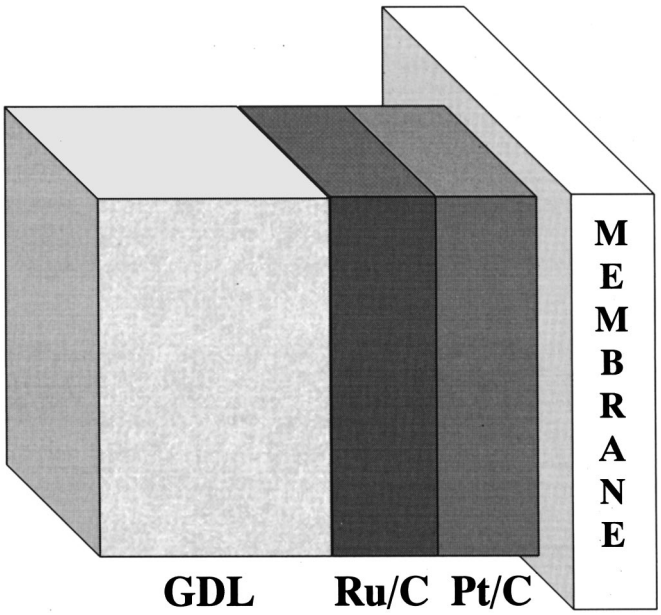

Figure 1. Diagram of the Ru-filtered anode. The feed gases pass through the GDL and come in contact with the Ru filter before reaching the Pt anode. The Ru filter acts as a chemical barrier on which O_2 oxidizes the CO present in the feed stream to CO_2, preventing a loss in the Pt anode performance due to CO poisoning.

conditions.[12] CO has been shown to have similar adsorption strengths onto Ru as Pt.[12,17-19] Thus, the slow H_2 kinetics of pure Ru would become an advantage, allowing a greater percentage of O_2 to oxidize CO_{ads} to CO_2 rather reacting with adsorbed hydrogen to form water. Pt catalyst is then placed after Ru to oxidize H_2 and maintain the high PEMFC performance.

The second objective was to characterize the mechanism of CO oxidation occurring within the Ru filter by varying the Nafion content (10 or 35 wt %) within it and its placement along the anode. The Ru filter can be placed between the gas diffusion layer (GDL) and Pt anode as shown in Fig. 1, or between the flow channels and the GDL. By varying the placement of the Ru filter, the role of Nafion electrolyte in CO oxidation could be determined.

Experimental

Development of Pt and Pt:Ru catalyst MEAs.—The method described in Patent no. 5,211,984 provides an outline for NCI and membrane electrode assembly (MEA) manufacture in this project.[20] The Pt and Pt:Ru (1:1 atomic ratio) catalysts were bonded to the Nafion 112 proton exchange membrane (PEM) in several steps. These steps included the formulation of the catalyst inks, application of the inks to decals, and transference of the dried catalyst ink from the decal to the membrane. Inks were prepared for Pt and Pt:Ru by adding the E-TEK catalyst to a solution of 5 wt % Nafion (DuPont).

The components of the ink were added to an appropriate size bottle (evacuated with helium to avoid sparking) and then stirred for a minimum of 8 h to ensure uniformity of the ink. Three-ply Teflon decals were weighed prior to applying the application of the ink. The ink was drawn across the surface of the Teflon decals using a Meyer rod. The loadings of 0.40 mg Pt/cm^2 (anode), 0.61 mg Pt:Ru/cm^2, and 0.50 mg Pt/cm^2 (cathode) were achieved. The coated decals were then dried in an oven at 105°C and ambient pressure for 10 min to remove any remaining alcohols from the ink.

To form an MEA with an active area of 50 cm^2, decals coated with an anode and cathode were placed on either side of a Nafion 112 membrane (proton form). The assembly was then hot-pressed for 2 min at 205°C. The assembly was cooled to room temperature before the decals were carefully pealed from the assembly, leaving an MEA.

Table I. Types of MEUs tested.

MEU name	Description
Pt (baseline)	0.4 mg Pt/cm^2 anode 0.5 mg Pt/cm^2 cathode Uncatalyzed Zoltek GDLs on anode and cathode
Pt:Ru	0.61 mg Pt:Ru/cm^2 anode 0.5 mg Pt/cm^2 cathode Uncatalyzed Zoltek GDLs on anode and cathode The atomic ratio of Pt to Ru in the Pt:Ru alloy is 1:1, resulting in an anode Pt loading of 0.4 mg/cm^2.
Pt + Ru (Ru filter)	0.4 mg Pt/cm^2 anode 0.5 mg Pt/cm^2 cathode 0.21 mg Ru/cm^2 coated Zoltek GDL on the anode Uncatalyzed Zoltek GDL on the cathode side

Development of the Ru filter.—Ru filters on both the catalyst and flow channel sides of the GDL were studied. Ru inks containing 35 and 10% Nafion solids by weight, respectively, were prepared in a similar method to Pt and Pt:Ru catalyst inks. The ruthenium ink was applied to the microlayer side of an uncatalyzed Zoltek GDL with a cross-sectional area of 50 cm^2. A Meyer rod was used to achieve a target loading of 0.21 mg Ru/cm^2. After the Ru/C catalyst was applied, the GDLs were dried at 105°C and ambient pressure for 10 min. Ru filters placed on the flow channel side of the GDL were prepared in a similar manner and with identical loadings.

Cell assembly and testing.—The three types of 50 cm^2 membrane-electrode units (MEUs) prepared and tested are shown in Table I.

The MEUs were placed in a 50 cm^2 cell. The cell was assembled and incubated for 4-8 h at ambient pressure, cell temperature of 70°C, an anode feed of hydrogen, a cathode feed of air, and a stoichiometric ratio (actual flow/stoichiometric flow required for a 1.0 A/cm^2 current) of 1.5 at the anode and 2.0 at the cathode. Single-cell performance curves were obtained under the conditions set in Table II.

An alternate test station was used to conduct trials using CO concentrations greater than 50 ppm (H_2, H_2 + 50 ppm CO, H_2 + 100 ppm CO, and H_2 + 200 ppm CO). The data attained on this station were consistent and reproducible, however, problems arising from excess water entering the test cell on these trials limit comparisons of this data to a qualitative nature.

Results and Discussion

Performance of the Ru filter.—Figures 2 and 3 show the performance of a Pt:Ru and Pt + Ru filter anode under five different anode feeds: (*i*) hydrogen, (*ii*) reformate; (*iii*) reformate + 2% O_2, (*iv*) reformate + 1% O_2, and (*v*) reformate + 0.5% O_2. In the case of Pt:Ru, as the amount of oxygen in the feed is reduced, the performance decreases in a continuous fashion. For a Pt + Ru anode, there is very little difference in performance between reformate + 2% O_2 and reformate + 1% O_2, but as the concentration of the oxygen in the reformate is reduced to 0.5%, there is a sudden drop in performance such that the performance curve resembles that of pure reformate. For conditions of 1-2% O_2 (by volume of H_2) addition to the reformate feed stream, the Pt + Ru filter performed better than the Pt:Ru alloy anode.

Figure 4 compares the cell performance of Pt, Pt:Ru, and Pt + Ru filter anodes under conditions of reformate + 1.0% O_2 bleed. Under these conditions, the Ru filter outperforms a Pt:Ru

Table II. Fuel-cell test conditions.

Pressure	1 atm (anode and cathode)
Cell temperature	70°C
Stoichiometric ratio (at 1 A/cm^2)	1.5 Anode (hydrogen) 2.0 Cathode (air)
Feedstreams	Anode: hydrogen, reformate, reformate + air bleed, H_2 + CO + air bleed Cathode: air
Dry reformate composition	40% H_2 20% CO_2 50 ppm CO balance N_2
Humidification	Complete humidification of anode and cathode gas streams for all trials.
Air bleed	0.5, 1.0, 2.0% O_2 (in the form of an air bleed relative to the volumetric flow of hydrogen in slm).
CO amounts	50 ppm in reformate 50, 100, 200 ppm in H_2

alloy anode of an identical loading by the greatest margin. At 0.6 V, the current density produced from the cell containing the Pt + Ru filter is almost double that of an identical cell using the Pt:Ru alloy. The Pt:Ru shows performance improvement over the plain Pt anode only at voltages below 0.5 V.

Conversely in Fig. 5, the cell performance of the Pt:Ru alloy for reformate + 0.5% O_2 shows the greatest tolerance to CO of the three anodes. At 0.6 V, the Pt:Ru cell provides 50% more current than the Pt + Ru filter. Both Ru-containing anodes do perform better than the pure Pt anode, but there is little benefit gained from using the Pt + Ru filter instead of a pure Pt anode. Similarly, in Fig. 6, with no air bleed in the reformate stream, the Ru filter shows performance resembling that of a pure Pt anode, while the Pt:Ru alloy anode exhibits some CO tolerance. In all cases these results were reproducible over several trials using different MEAs of identical loadings.

Thus, without sufficient oxygen in the anode feed to oxidize CO to CO_2, the CO penetrates the Ru filter and poisons the Pt region of the anode. A representation of this is shown in Fig. 7 where the shading indicates the relative concentration of CO in the anode. As CO is oxidized, the concentration of CO decreases as it passes through the filter region. Figure 7a is indicative of adding 1-2% O_2 to the reformate stream. All CO is oxidized from the feed stream

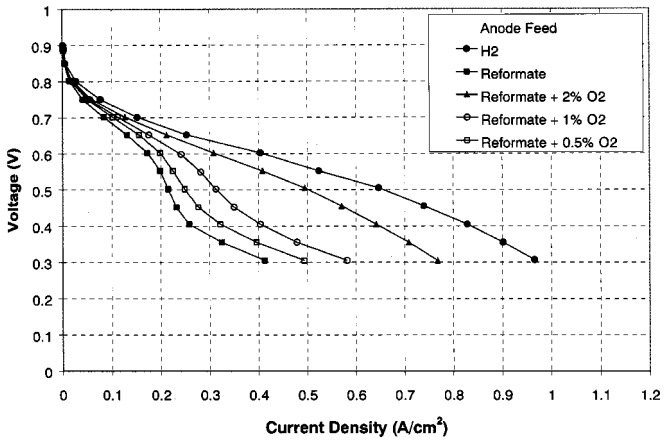

Figure 2. Single-cell performance comparison of Pt:Ru for various anode feeds. $P = 1$ atm, $T = 70$°C.

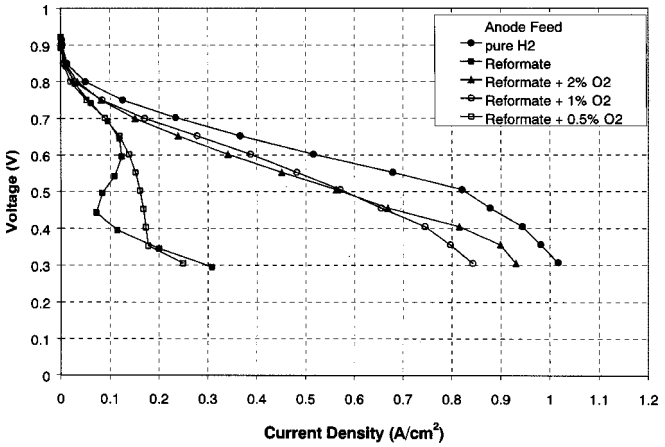

Figure 3. Single-cell performance comparison of the Pt + Ru filter for various anode feeds. $P = 1$ atm, $T = 70$°C.

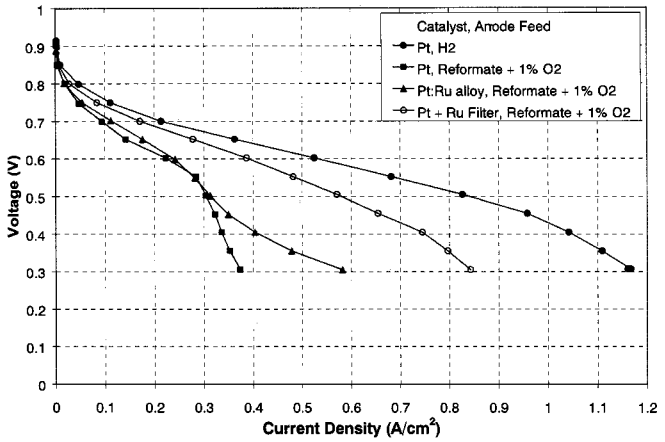

Figure 4. Single-cell performance comparison of Pt, Pt:Ru, and Pt + Ru filter for an anode feed of reformate + 1% O_2 bleed. $P = 1$ atm, $T = 70$°C.

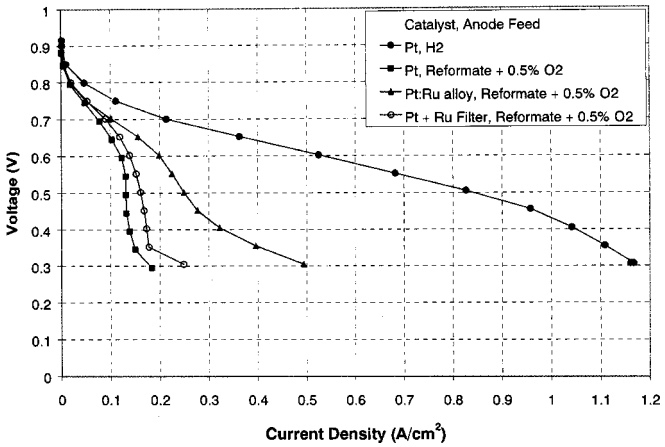

Figure 5. Single-cell performance comparison of Pt, Pt:Ru, and Pt + Ru filter for an anode feed of reformate + 0.5% O_2 bleed. $P = 1$ atm, $T = 70$°C.

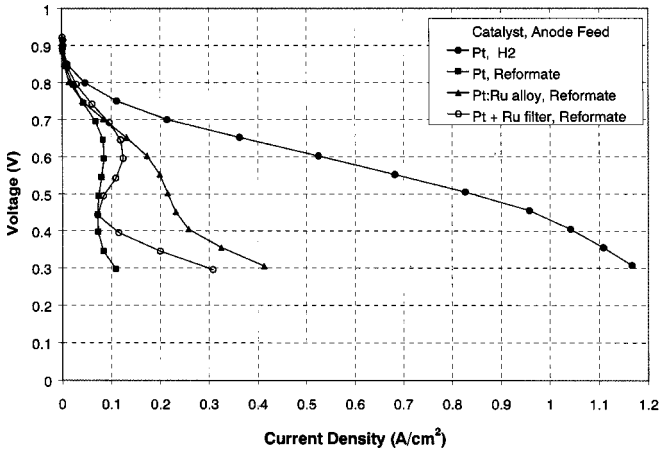

Figure 6. Single-cell performance comparison of Pt, Pt:Ru, and Pt + Ru filter for an anode feed of reformate. $P = 1$ atm, $T = 70°C$.

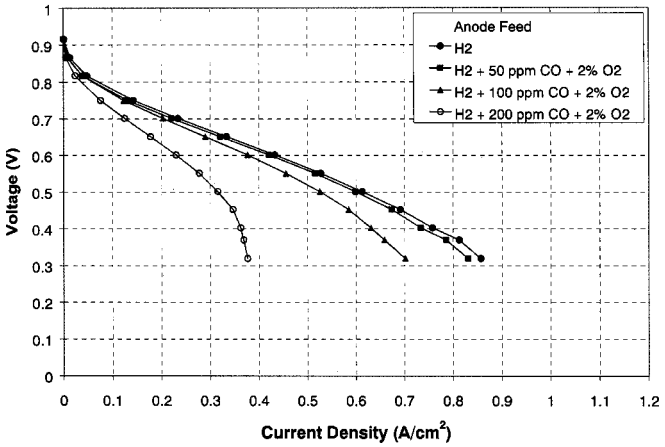

Figure 8. Single-cell performance comparison of the Pt + Ru filter for an anode feed consisting of hydrogen + 2% O_2 + various CO concentrations. $P = 1$ atm, $T = 70°C$.

before it reaches the Pt portion of the electrode and as a result, the cell operates with minimal performance losses. Figure 7b illustrates that when the Ru filter fails to oxidize CO before it diffuses through the filter region, the remaining CO then encounters the pure Pt electrode where it poisons the Pt through the reaction shown in Eq. 1.

A decrease of the O_2 concentration in the anode feed (Fig. 3) or an increase in the CO concentration in the anode feed stream results in the eventual failure of the Pt + Ru filter anode. Figure 8 shows the performance of the Ru filter anode when using an anode feed of hydrogen, 2% O_2, and various levels of CO. When 50 ppm CO is present, there is almost no reduction in performance (0.43-0.42 A/cm^2 at 0.6 V). This is inconsistent with the same amount of CO contained in a reformate stream (Fig. 3) and can be attributed to the dilution of hydrogen in the reformate stream. (Completely humidified at 70°C, reformate + 2% O_2 in the form of an air bleed contains 28% H_2 by volume compared to a 70 vol % H_2 for an H_2 + 2% O_2 feed.) Because hydrogen must diffuse through the Ru filter in order to react on the Pt electrode, additional diffusional resistance accounts for the remaining performance losses compared to the perfomance of a baseline MEA with an anode feed of pure hydrogen. As the CO level increases to 100 ppm, the current density decreases from 0.42 to 0.38 A/cm^2 at 0.6 V, indicating that the limit of the Ru filter may have been reached. At 200 ppm CO, the drop in performance is much larger (0.38-0.23 A/cm^2 at 0.6 V). In this case, not all the CO is oxidized in the Ru filter region, resulting in the poisoning of the Pt portion of the electrode. This trend is qualitatively similar to the reduction of the air bleed as shown in Fig. 3.

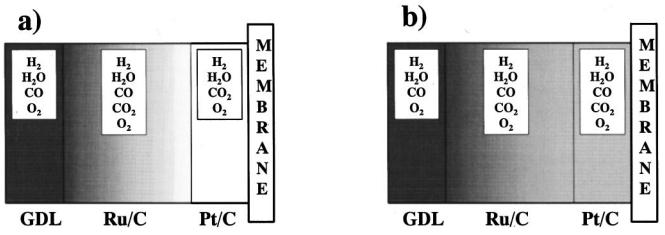

Figure 7. A schematic representation of the species present in the various regions of the Pt + Ru filter anode. The shading indicates the relative concentration of the CO in each region (the lighter the shade, the lower the concentration). In (a) all CO is oxidized within the filter region and the Pt catalyst receives CO-free gas. In (b) the concentration of CO in the inlet gas is too great to be completely oxidized within the filter and poisons the anode catalyst.

Mechanism of the Ru filter.—Equations 2 and 5 present two different methods for CO oxidation. In the mechanism shown in Eq. 2, the oxidation of CO generates H^+, whereas the CO oxidation described in Eq. 5 produces no ions. Thus, by removing the electrolyte that allows H^+ to diffuse away from the reaction site, CO oxidation through the mechanism in Eq. 2 can be effectively prevented. This enables the CO oxidation through Eq. 5 to be isolated and analyzed.

The isolation of the Ru filter was achieved by applying it to the flowfield side of the electrolyte, thus separating it from the Pt electrode by the GDL. The Toray GDL contained no Nafion electrolyte and was sufficiently thick (175 μm) to provide adequate separation from the Pt electrode. To further characterize these two mechanisms, Ru filters containing 10 wt % Nafion were tested on both the membrane and flowfield sides of the GDL.

Figure 9 shows the effect of varying the Nafion content within the Ru filter and the effect of the placement of the Ru filter for an anode feed of reformate +2% O_2. Of the four types tested, the Ru filter placed on the membrane side of the GDL and containing 35 wt % Nafion showed the greatest performance. Both Ru filter types

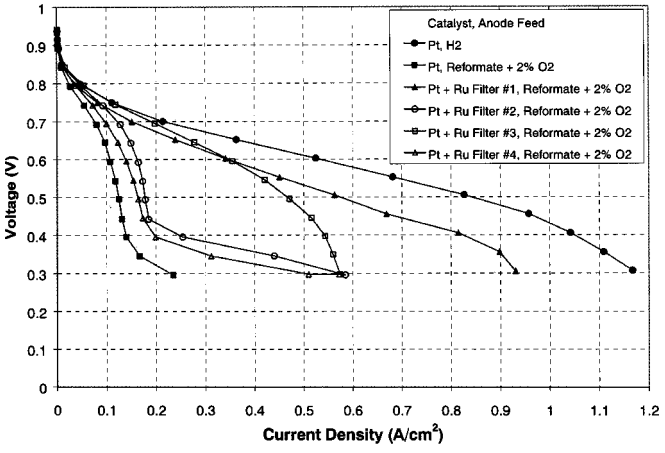

Figure 9. Single-cell performance comparison of the Pt + Ru filter for an anode feed of reformate + 2% O_2. $P = 1$ atm, $T = 70°C$. The filter configurations are defined as follows: filter no. 1 (—▲—) contains 35 wt % Nafion and is placed on the membrane side of the GDL; filter no. 2 (—○—) contains 35 wt % Nafion and is placed on the flowfield side of the GDL; filter no. 3 (—□—) contains 10 wt % Nafion and is placed on the membrane side of the GDL; filter no. 4 (—△—) contains 10 wt % Nafion and is placed on the flowfield side of the GDL.

placed on the flowfield side of the GDL provide almost no benefit over the pure Pt anode, providing 0.14 and 0.16 A/cm^2 at 0.6 V compared to 0.34 A/cm^2. The Ru filter on the membrane side of the GDL and containing 10 wt % Nafion performed similar to the 35 wt % filter for 0.6 V and above, but the lack of electrolyte present most likely induced H^+ diffusion limitations at a lower current density.

Thus, it is believed that the following mechanism is occurring in the ruthenium filter for a fully humidified fuel stream containing oxygen, hydrogen, and carbon monoxide[21-33]

$$Ru + H_2 \leftrightarrow 2H_{ads} \quad [7]$$

$$Ru + CO \leftrightarrow CO_{ads} \quad [8]$$

$$O_2 + 2Ru \leftrightarrow 2\ O_{ads} \quad [9]$$

$$H_{ads} + O_{ads} \rightarrow OH_{ads} + Ru \quad [10]$$

$$CO_{ads} + OH_{ads} \rightarrow CO_2 + H^+ + 2Ru + e^- \quad [11]$$

$$H^+ + e^- + OH_{ads} \leftrightarrow H_2O + Ru \quad [12]$$

$$CO_{ads} + O_{ads} \rightarrow CO_2 + 2Ru \quad [13]$$

$$H_{ads} \rightarrow H^+ + e^- + Ru \quad [14]$$

Reactions 7-9 represent the adsorption of species onto the Ru catalyst. Reaction 10 represents an intermediate reaction on Ru resulting in the formation of OH_{ads}. Like on Pt, oxygen dissociatively adsorbs on Ru to form O_{ads}.[25,29,32] Reactions 11-14 represent competing desorption reactions on the Ru catalyst. Equation 13 is well documented as following Langmuir-Hinshelwood kinetics on Pt and Ru.[34,35] Of the desorption reactions, Eq. 11 and 13 are desired as they result in the oxidation of CO_{ads}. The above-described mechanism is not a comprehensive list of all reactions occurring within the anode region. It focuses on those reactions that lead to CO oxidation. For example, evidence has been found that H_2O_2 is formed as an intermediate during oxygen reduction at overpotentials as low as 0.5 V.[36] However, H_2O_2 breaks back down to oxygen-containing compounds at or even before reaching the catalyst surface.[2,5,13]

The rationale for the placement of the filter on the flowfield side of the GDL is that if the oxidation of CO_{ads} were to proceed via Eq. 11, a three-phase interface (anode gas, Nafion, and Pt/C) is not needed in the catalyst mixture because there are no ions or electrons to be transported away from the reaction site. Because some Nafion is necessary in the Ru filter to act as a binder, the Ru filter was merely placed on the flowfield side of the GDL. There is no Nafion electrolyte in the GDL to allow proton transport and the GDL is sufficiently thick ($\sim$5 mil). Without the Nafion electrolyte as a conduit and because of the long distance that the protons must travel, the formation of CO_2 through Eq. 11 does not occur to any significant extent and the reaction shown in Eq. 13 is isolated. Thus, the amount of CO_{ads} oxidized through the reaction shown in Eq. 13 is also insufficient to provide the levels CO tolerance shown in both Fig. 3 and 8. This is consistent with literature, where it is also shown that Ru is one of the least active metals for this method of CO oxidation at the oxygen partial pressures used in these experiments.[25,29]

Further evidence of the role of Nafion content in the membrane is shown for the cases in Fig. 9. Significant CO oxidation only occurs when the Ru filter is placed adjacent to the Pt anode. This is evidence that protons are formed as product of CO oxidation. The Nafion electrolyte is the necessary conduit for the protons to move away from the reaction site and when this conduit is present, cell performance increases when all other parameters are unchanged. The increased performance under conditions of increased Nafion content shown in Fig. 9 is further proof that CO_{ads} oxidation is occurring by the mechanism that involves the formation of protons which is described in Reaction 11. Thus, Reaction 13 does occur to a small extent as evidenced by the slight increase in performance when the filter is placed on the flowfield side of the GDL, but the rate of Reaction 11 is far greater than Reaction 13 when the filter is ionically connected to the MEA.

The hydroxyl group in Reaction 11 can be formed either from oxygen through Reactions 9 and 10 or from water through Reaction 12. In fact, both are occurring within an Ru filter when it is adjacent to the Pt anode. The mechanism primarily responsible for the CO tolerance of the Pt:Ru alloy is comprised of Reactions 11 and 12. Figure 6 shows that in the absence of an air bleed, there is only a small performance increase relative to a pure Pt anode. Thus, the formation of OH_{ads} through the reverse of Reaction 12 is not the primary source of the hydroxyl species needed for Eq. 11. It is clear that the Pt:Ru alloy performs better under reformate conditions. Gasteiger[11,12,14,30] performed extensive research on this mechanism and found that while OH_{ads} is indeed formed at lower potentials on Ru than Pt, the hydroxyl group also forms a stronger bond on pure Ru than a 1:1 atomic ratio Pt:Ru alloy, resulting in higher CO oxidation potentials on pure Ru than on the Pt:Ru alloy. It can be speculated that the rate of formation of OH_{ads} in the Ru filter is equivalent to that in the Pt:Ru alloy.[30] However, it is clear from Fig. 6 that without the presence of oxygen in the anode feed that only a fraction of the CO is oxidized in the Ru filter and that the remaining CO poisons the Pt anode.

Thus, the primary method by which CO tolerance is achieved by the Ru filter is by the formation of OH_{ads} from oxygen in the air bleed. The explanation of near complete oxidation of CO at concentrations up to 100 ppm is the result of Reactions 9-11. That near CO-free performance is achieved with the addition of 2% O_2 to the anode feed while the filter provides almost no benefit under reformate conditions is evidence that Reactions 9-11 are the primary means of CO oxidation within the filter region.

The key is that O_{ads} forms OH_{ads} before reacting with a second proton to form water. This is where the benefit of the Ru filter lies. The oxidation of H_{ads} occurs within the filter according to Reaction 14 forming H^+. Because the kinetics of hydrogen adsorption on Ru is several orders of magnitude slower than on Pt, there is a lower concentration of H_{ads} in the filter region and more of an opportunity for CO_{ads} to react with OH_{ads}, resulting in the formation of CO_2. The bulk of the hydrogen oxidation occurs in the Pt region. However, protons must be present within the Ru filter for Reaction 10 to occur, and because these protons will also shift Reaction 12 toward the formation of H_2O, there is a limit to the benefit of the Ru filter.

Conclusions

For an anode feed stream consisting of reformate (containing 50 ppm CO) and 1-2% oxygen, the Pt + Ru filter electrode shows increased CO tolerance compared to a Pt:Ru alloy containing similar amounts of Pt and Ru. For CO concentrations up to 100 ppm and 2 vol % O_2, the Pt + Ru filter anode also shows superior performance. It is likely that the oxidation of the CO within the Ru filter is primarily due to oxygen reacting to form OH_{ads}, which then electrochemically reacts with CO_{ads} to form CO_2 and protons.

However, with insufficient oxygen ($<$1 vol %) or too much CO ($>$100 ppm), not all CO is oxidized in the Ru filter. Remaining CO reaches and then poisons the Pt region of the Pt + Ru filter anode. As a result, cell performance under those conditions is worse than the Pt:Ru alloy anode.

Because benefits of the Ru filter occur at high levels air bleed (2% O_2) and the Pt:Ru alloy provides CO tolerance even without air bleed, it is suggested that the anode configuration that would provide optimal CO tolerance would consist of an Ru filter placed in front of and adjacent to a Pt:Ru alloy.

Acknowledgments

The authors acknowledge the financial support from the National Institute of Standards and Technology under cooperative agreement no. 70NANB8H4039.

The University of South Carolina assisted in meeting the publication costs of this article.

References

1. H. P. Dhar, L. G. Christner, A. K. Kush, and H. C. Maru, *J. Electrochem. Soc.*, **133**, 1574 (1986).
2. H. F. Oetjen, V. M. Schmidt, U. Stimming, and F. Trila, *J. Electrochem. Soc.*, **143**, 3838 (1996).
3. H. P. Dhar, L. G. Christner, and A. K. Kush, *J. Electrochem. Soc.*, **134**, 3021 (1987).
4. B. N. Grgur, N. M. Markovic, and P. N. Ross, *J. Electrochem. Soc.*, **146**, 1613 (1999).
5. R. J. Bellows, E. P. Marucchi-Soos, and D. T. Buckley, *Ind. Eng. Chem. Res.*, **35**, 1235 (1996).
6. M. Iwase and S. Kawatsu, in *Proton-Conducting Membrane Fuel Cells*, A. R. Landgrebe, S. Gottesfeld, and G. Halpert, Editors, PV 95-23, pp. 12-23, The Electrochemical Society Proceedings Series, Pennington, NJ (1995).
7. M. Watanabe, H. Igarashi, and T. Fujino, *Electroanal. Chem.*, **67**, 1194 (1999).
8. B. N. Grgur, N. M. Markovic, and P. N. Ross, Jr., in *Proton Conducting Membrane Fuel Cells*, S. Gottesfeld, T. F. Fuller, and G. Halpert, Editors, PV 98-27, p. 176, The Electrochemical Society Proceedings Series, Pennington, NJ (1998).
9. A. B. Anderson, E. Grantscharova, and P. Schiller, *J. Electrochem. Soc.*, **142**, 1880 (1995).
10. M. Gotz and H. Wendt, Fuel Cell Seminar Abstracts, Palm Springs, CA, p. 616, Nov 16-19, 1998.
11. H. A. Gasteiger, N. M. Markovic, and P. N. Ross, Jr., *J. Phys. Chem.*, **99**, 8290 (1995).
12. H. A. Gasteiger, N. M. Markovic, and P. N. Ross, Jr., *J. Phys. Chem.*, **99**, 16757 (1995).
13. R. J. Bellows, E. Marucchi-Soos, and R. P. Reynolds, *Electrochem. Solid-State Lett.*, **1**, 69 (1998).
14. K. Wang, H. A. Gasteiger, N. M. Markovic, and P. N. Ross, Jr., *Electrochim. Acta*, **41**, 2587 (1996).
15. M. T. M. Koper, J. J. Lukkien, A. P. J. Jansen, and R. A. van Santen, *J. Phys. Chem.*, **103**, 5522 (1999).
16. V. M. Schmidt, H.-F. Oetjen, and J. Divisek, *J. Electrochem. Soc.*, **144**, L237 (1997).
17. C. T. Campbell, G. Ertl, H. Kuipers, and J. Segner, *J. Chem. Phys.*, **73**, 5862 (1980).
18. T. Madey, A. Engelhardt, and D. Menzel, *Surf. Sci.*, **48**, 304 (1975).
19. S. J. Lee, S. Mukerjee, E. A. Ticianelli, and J. McBreen, *Electrochim. Acta*, **44**, 3283 (1999).
20. M. S. Wilson, U.S. Pat. 5,211,984 (1993).
21. S. H. Oh and R. M. Sinkevitch, *J. Catal.*, **142**, 254 (1993).
22. N. M. Markovic, T. J. Schmidt, B. N. Grgur, H. A. Gasteiger, R. J. Behm, and P. N. Ross, *J. Phys. Chem.*, **103**, 8568 (1999).
23. N. M. Markovic, B. N. Grgur, C. A. Lucas, and P. N. Ross, *J. Phys. Chem. B*, **103**, 487 (1999).
24. K. Bleakley and P. Hu, *J. Am. Chem. Soc.*, **121**, 7644 (1999).
25. C. Zhang, P. Hu, and A. Alavi, *J. Am. Chem. Soc.*, **121**, 7931 (1999).
26. E. Yeager, *J. Mol. Catal.*, **38**, 5 (1986).
27. E. Yeager, *Electrochim. Acta*, **29**, 1527 (1984).
28. A. Alavi, P. J. Hu, T. Deutsch, P. L. Silvestrelli, and J. Hutter, *Phys. Rev. Lett.*, **80**, 3650 (1998).
29. H.-I. Lee, G. Praline, and J. M. White, *Surf. Sci.*, **91**, 581 (1980).
30. H. A. Gasteiger, N. Markovic, P. N. Ross, and E. J. Cairns, *J. Phys. Chem.*, **98**, 617 (1994).
31. P. Ferreira-Aparicio, A. Guerrero-Ruiz, and I. Rodriguez-Ramos, *Appl. Catal., A*, **170**, 177 (1998).
32. P. Ferreira-Aparicio, I. Rodriguez-Ramos, J. A. Anderson, and A. Guerrero-Ruiz, *Appl. Catal., A*, **202**, 183 (2000).
33. P. Freni, G. Calogero, and S. Cavallaro, *J. Power Sources*, **87**, 28 (2000).
34. P. J. Berlowitz, C. H. F. Peden, and D. W. Goodman, *J. Phys. Chem.*, **92**, 5213 (1998).
35. R. Imbihl, M. P. Cox, and G. Ertl, *J. Chem. Phys.*, **83**, 1578 (1985).
36. N. M. Markovic, T. J. Schmidt, V. Stamenkovic, and P. N. Ross, *Fuel Cells*, **1**, 105 (2001).